11th World Congress on Computational Mechanics (WCCM XI)
5th European Conference on Computational Mechanics (ECCM V)
6th European Conference on Computational Fluid Dynamics (ECFD VI)
E. Oñate, J. Oliver and A. Huerta (Eds)

SYSTEM FOR RECONSTING IMAGES OF INTERNAL DEFECTS BY INVERSE PROBLEM SOLVING

Yoshihiro Nishimura[1], Katsumi Fukuda[2], Takayuki Suzuki[1] and Masatoshi Fukuta[2]

[1] National Institute of Advanced Science and Technology
1-2-1 Namiki Tsukuba Ibaraki 305-8564 Japan
e-mail: nishimura.yoshihiro@aist.go.jp, e-mail: suzuki-taayuki@aist.o.jp
[2] Tokyo National College of Technology
1220-2 Kunugida Hachioji Tokyo, 193-0997 Japan
e-mail: fukuda@tokyo-ct.ac.jp, e-mail: as13605@tokyo-ct.ac.jp

Key words: Probe Array, Inverse Problem, Truncated Singular Value Decomposition.

Abstract. Ceramic materials are unreliable for manufacturing large structural components because they are likely to have fatal internal defects and their fracture responses are much faster and more drastic than those of metal materials. Ultrasonic Testing, particularly imaging of internal defects, is necessary for reliable use. 3D scanning systems and programs were developed to derive images of internal defects. Truncated Singular Value Decomposition, an Inverse-problem-solving method, was conducted to reconstruct internal defect images. This study investigated what factors (e.g., frequency and number of piezoelectric elements) affect the reconstructed defect images.

1 INTRODUCTION

Ceramic materials, such as silicon nitride, have superior rigidity and heat resistance than metal material and are expected to be applied in fields such as metal industries and high-precision electronics industries. However, ceramic materials are likely to contain internal defects and they fracture very fast, so it is important to detect internal defects.

Ultrasonic Testing (UT), a one of non-destructive test method, is useful for maintaining the safety and soundness of airplanes, railroads, playground equipment, and other social infrastructures. Phased arrays, which have become popular for probe arrays recently, are convenient NDT systems for deriving images of internal defects by electronically scanning inside material.

However, the acoustic velocity of ceramics material is higher and the wavelength longer than those of metal materials, so the near-field range becomes shorter than that of metal materials. Therefore, large-aperture, long focal length piezoelectric elements are required when inspecting a defect deep in a large ceramic structure. The acoustic velocity of Silicon

Nitride (SN) is 9,000 m/s to 12,000 m/s and one half to twice the acoustic velocity of steel. Acoustic lenses with focal lengths of 600 mm to 800 mm are required for use as a point focus lens, but such lenses are difficult to manufacture. High acoustic velocity makes the wave length longer, but the resolution of images depends on the wavelength within the inspected sample as well.

A popular frequency for a UT probe array is 5 MHz, and its wavelength in SN is 18 mm to 24 mm. Resolutions of phased-array methods and aperture synthesis depend on wavelength. Inverse problem solving is useful for achieving better resolution of defect images. Inverse problem solving must solve the inverse matrix of the response function. Such a response function matrix is often singular, so the inverse matrix of response function cannot be derived due to the limitation of numerical methods. Truncated Singular Value Decomposition Methods can address this problem. Its performance depends on the frequency, number of elements, and acoustic velocity of materials. Relations among them have to be considered.

2 CONVENTIONAL ULTRASONIC INSPECTION

An ultrasonic wave from a piezoelectric oscillator enters an object and reflects from internal defects and the bottom edge as depicted in Fig. 1. Internal defect position and size can be measured from time series of waveform data received by the probe. It can be used for metal materials, nonmetallic substances, and surface defects.

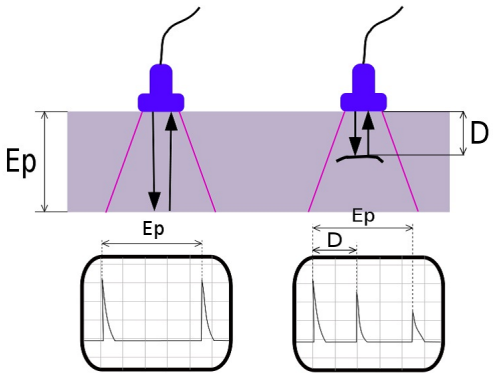

Figure 1: Ultrasonic inspection

3 PROBE ARRAY

A array (Fig. 2) has a probe with multiple piezoelectric elements in line. Each element's pulsing-voltage and delay-time can be configured individually. Phased-array methods can focus at any point inside an inspected sample by setting the pulsing time properly. The intensity of reflection at any focus point can be obtained by summing the time series of waveforms with an appropriate time delay. Thus, scanning a cross section within an

inspected sample soon reconstructs cross section images including internal defects. Moving the probe array in the Y direction produces 3-D images within the sample (Fig. 3). A 2-D scanning probe can reproduce 3-D images within a sample[1].

However, scanning all cross sections generates large reverberations and takes much time. Therefore, actual usages of phased arrays are limited to linear scans, sector scans or Dynamic Depth Focusing (DDF). Unfortunately, these imaging systems cannot provide us resolution far from the focus that is as good as at the focus point. However, aperture synthesis and inverse problem solving address these issues.

Flush focus, which was proposed by D.Braconier, pulses all elements simultaneously and generates plane waves. Cross section images can be produced using aperture synthesis from time series data received by each element. Inverse problem solving derives internal defect images by solving the inverse matrix of the response function of the probe-array system.

Probe-array specifications are shown in Table 1.

Table 1: Specification of probe array

Dimensions of probe	25 mm x 25 mm x 50 mm
Dimensions of elements	0.4 mm x 13 mm
Pitch of elements	0.5 mm
Number of channels	32
Operation frequency	5.0 MHz

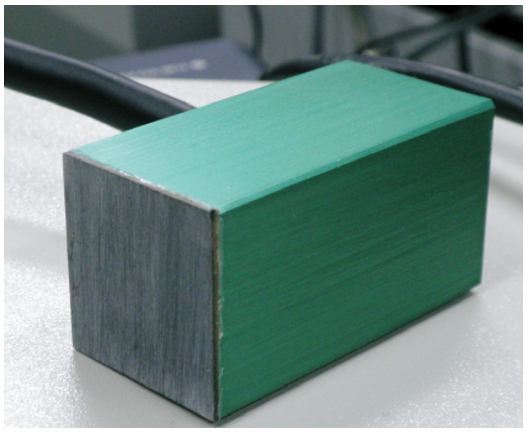

Figure 2: Array probe

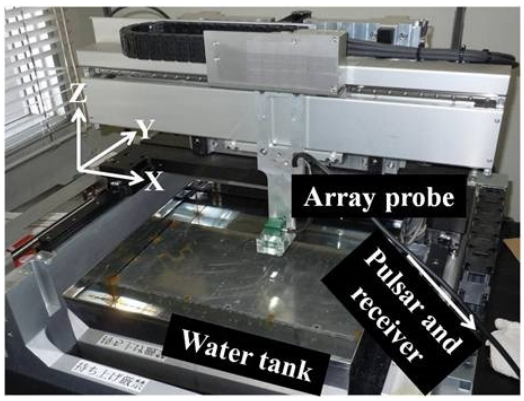

Figure 3: Measuring device

4 NDT-SYSTEM

Figure 4 presents our Non-destructive Testing System[2]. Our system consists of a 3-D scanner, probe array, a pulser/receiver, and a PC with an AD converter (Fig. 3). An array probe can be positioned precisely on an inspected sample by a 3-D scanner. The probe array operates at 5MHz. The acoustic velocity i SN is 10870 m/s and the wavelength in SN is 2.2 mm.

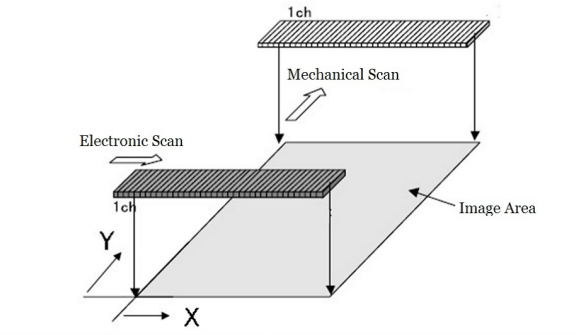

Figure 4: Phased array

5 Truncated Singular Value Decomposition Method

Suppose that an acoustic signal is emitted from a probe array and that the return signal is observed as illustrated in Fig. 5.

If all elements pulse simultaneously, the acoustic signal can be thought to be a plane wave. The signal $f(t, x_0)$ emitted from $\vec{x_0} = (x_0, 0)$ on the probe is described as $f(t, x_0) = f(t)$. Eq. 1 expresses the signal $v(t, x_1, z_1)$ observed at (x_1, z_1). The signal $u(\vec{x_2}, t)$ observed at $(x_2, 0)$ is derived by integrating the signal reflected from within the sample with respect to (x_1, z_1) over the whole sample as described in Eq. 2. $\rho(x_1, z_1)$ is a distribution function of the acoustic reflection coefficient. Eq. 3 expresses the response function of the probe array system[3].

$$v(t, x_1, z_1) = f(t - \frac{z}{c}) \tag{1}$$

$$u(x_2, t) = \int \rho(x_1, z_1) h(x_1 - x_2, z_1, t) dx_1 dz_1 \tag{2}$$

$$h(x, t) = \frac{f\left(t - \frac{z}{c} - \frac{\sqrt{z^2+x^2}}{c}\right)}{\sqrt{z^2 + x^2}} \tag{3}$$

Eq. 2 can be rewritten as Eq. 4 by Fourier transformation. $U(X, t)$, $H(X, z, t)$, and $P(X, z)$ are Fourier-transformed from $u(x, t)$,$h(x, z, t)$, and$\rho(x, z)$ on x.

$$U(X,t) = \int H(X,z_1,t)P(X,z_1)dz_1 \tag{4}$$

The matrix H can be broken as $H = A\Lambda B$. Here, A and B are orthogonal matricses and Λ is a diagonal matrix. $A = (\vec{a}_1\vec{a}_2\cdots)$, $B = (\vec{b}_1\vec{b}_2\cdots)^T$ and $\Lambda = diag(\lambda_1\lambda_2\cdots)$. $\lambda_i(i = 1, 2, \cdots)$ are singular values. $\lambda_1 \geq \lambda_2 \geq \cdots \lambda_n$ as well. Eq. 4 can be rewritten as Eq. 5. Here, $\vec{P}_X = \{P(X,z)\}$ and $\vec{U}_X = \{U(X,t)\}$.

$$\vec{U}_X = H\vec{P}_X = A\Lambda B^T\vec{P}_X \tag{5}$$

The reflection coefficient vector $\vec{P}_X$ can be solved using Singular Value Decomposition as expressed in Eq. 6.

$$\vec{P}_X = \frac{\vec{a}_1 \cdot \vec{U}_X}{\lambda_1}\vec{b}_1 + \frac{\vec{a}_2 \cdot \vec{U}_X}{\lambda_2}\vec{b}_2 + \cdots \frac{\vec{a}_n \cdot \vec{U}_X}{\lambda_n}\vec{b}_n \tag{6}$$

If n is large enough, $(\vec{a}_n \cdot \vec{U}_X)/\lambda_n$ should mathematically converge to 0. More terms of $(\vec{a}_n \cdot \vec{U}_x)/\lambda_n$ will improve image quality. It doesn't go do so in probe-array systems. λ_n becomes less than the minimum number δ of double precision computations when n is large enough. It means singularity of response function matrix. $(\vec{a}_n \cdot \vec{U}_X)/\lambda_n$ will actually make the function divergent and cannot produce an apropriate defect image.; that is why higher degrees of k (truncation index) of terms should be truncated. The concept is Truncated Singular Value Decomposition.

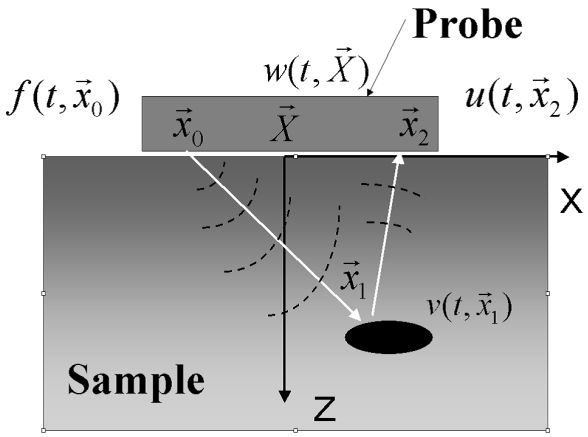

Figure 5: Probe-array and sample

6 Calculation of Numerical Model

Figures 6 (a), (b), (c), (d) compare reconstruction methods. Figure 6 (b) presents an image reconstructed from a numerical model Figs.6 (a) by aperture synthesis. Aperture synthesis is a numericaly stable reconstruction method, and its resolution depends on pulse width but accompanies artifacts around defects coming from image reconstruction itself. Figure 6 (c) presents a result calculated using the inverse matrix of the response function. The singularity of the response function matrix produced a divegent image. Figure 6 (d) presents a result calculated using TSVD with an apropriate truncation index k. TSVD numerically divergence and successfully produced an image of defect.

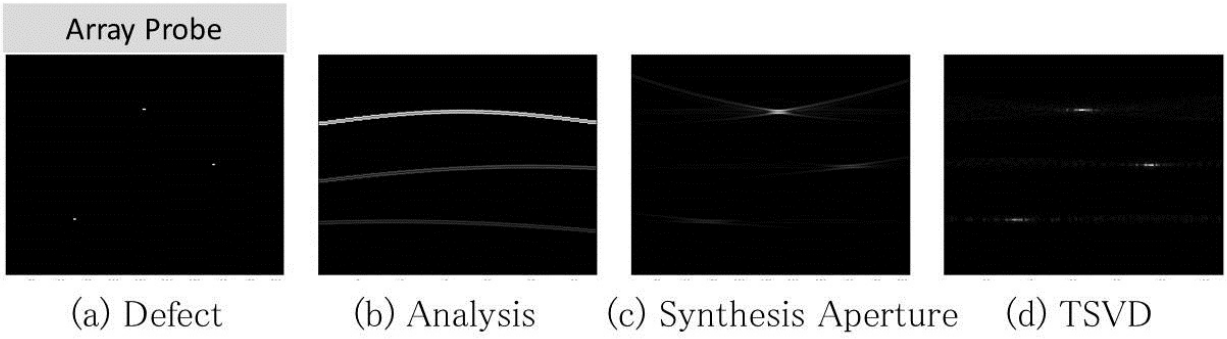

Figure 6: Defect image reconstructed

Figures 7 presents sample dimensions and effects of truncation index k. Two-slit defect images seem clear as truncation index k increases. Images cannot be improved than at beyond truncation index k=1024.

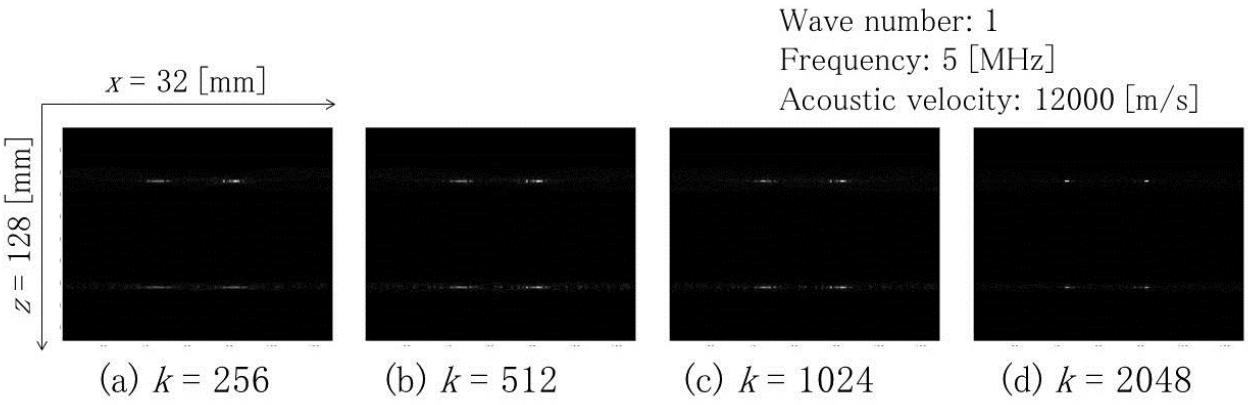

Figure 7: Images of deep defects in SN sample reconstructed using TSVD

7 Experiment result

TSVD was applied to an SN sample. Figures 8 (a), (b), and(c) present an samples dimensions, and images reconstructed by synthesis aperture and TSVD. Slit defect-images were successfully reconstructed.

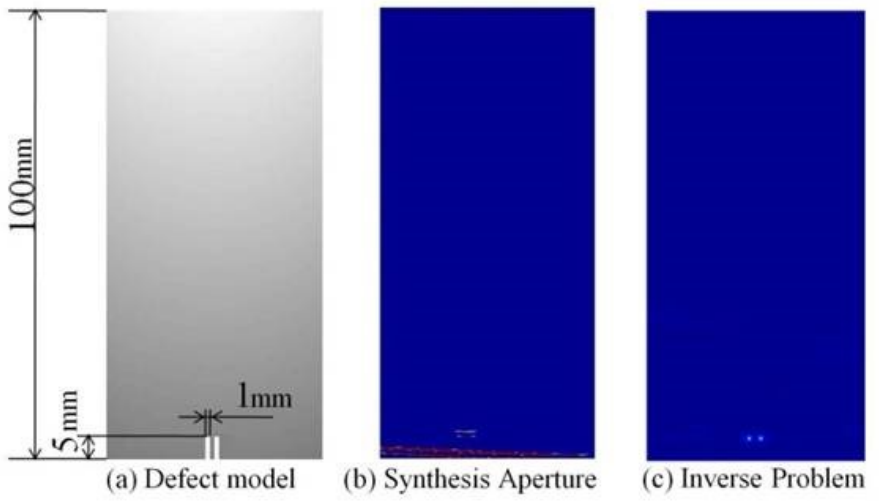

Figure 8: Images of deep defects in SN sample reconstructed using TSVD

8 CONCLUSIONS

- It was theoretically shown that the TSVD method could reproduce a clear defect image than the synthetic-aperture method.
- TSVD was applied to actual experiment data and successfully reconstructed defect images.

REFERENCES

[1] Y. Nishimura, T. Suzuki, N. Kondo, H. Kita and K. Hirao. Study of Defect Inspection in Ceramic Materials Using UT an X-Ray. JSAEM Studies in Applied Electromagnetics and Mechanics, 14, pp.145-146, 2011.

[2] Y. Nishimura, T. Suzuki, K. Fukuda and N. Saito. Visualization of Internal Defects in Ceramic Products using UT Probe Array. Proceedings of the 36th International Conference on Advanced Ceramics and Composites, -, pp. -, August 2012.

[3] Y. Nishimura, T. Suzuki, K. Fukuda, M. Ishii and N. Saito. Image Reconstruction of Defects 100 mm deep within SN Sample using Inverse Solving. Proceedings of 2012 IEEE International Ultrasonics Symposium, -, pp, -, June 2013.